

Synthesis of azobenzene-functionalized star polymers via RAFT and their photoresponsive properties

Md. Zahangir Alam, Akihisa Shibahara, Tomonari Ogata, Seiji Kurihara*

Department of Applied Chemistry and Biochemistry, Kumamoto University, Kurokami 2-39-1, Kumamoto 860-8555, Japan

ARTICLE INFO

Article history:

Received 1 April 2011

Received in revised form

17 June 2011

Accepted 19 June 2011

Available online 25 June 2011

Keywords:

Star polymer

RAFT polymerization

Azobenzene molecules

ABSTRACT

Azobenzene-functionalized star polymers were synthesized by reversible addition–fragmentation chain transfer (RAFT) polymerization. First, azobenzene-functionalized linear macro chain transfer agents (Macro-CTA) were synthesized by RAFT polymerization of 6-[4-(4'-Methoxyphenylazo)phenoxy]hexylmethacrylate (MAz6Mc) using 2-(2'-cyanopropyl)dithiobenzoate (CPDB) as RAFT agent in presence of AIBN as initiator in anisole. Subsequently, star azopolymers were synthesized by polymerization of a difunctional azomonomer, BMA2Az, with resultant Macro-CTA in presence of AIBN as initiator in anisole. Star azopolymers were characterized by GPC and spectroscopic methods. Thermal properties of star azopolymers were determined by DSC and TMA. Molecular weight versus conversion and molecular weight versus polymerization time attest to living polymerization characteristics. Photoisomerization behaviors of star azopolymers were studied by irradiation of both UV and visible light. Surface relief gratings were inscribed on star azopolymer films upon exposure to an interference pattern of (RCP + RCP) Ar⁺ laser. A diffraction efficiency of 20% was obtained by exposure of Star-8 K(2.6 K) polymer film to an (RCP + RCP) Ar⁺ laser for about 30 min. Surface relief grating structures were investigated by AFM and polarized optical microscopy.

© 2011 Elsevier Ltd. All rights reserved.

1. Introduction

Star-shaped polymers are defined as polymers composed of multiple polymer chains linked to a central core. They have attracted great attention because of their unique properties leading to important applications [1–3]; these include lower melting points, lower bulk and solution viscosities and superior mechanical properties due to their more compact structure compared to their linear analogues of similar molecular weights [4–10]. Star polymers are also capable of possessing a higher degree of end group functionality compared to linear polymers of similar molecular weight, enabling their use in many specialized applications.

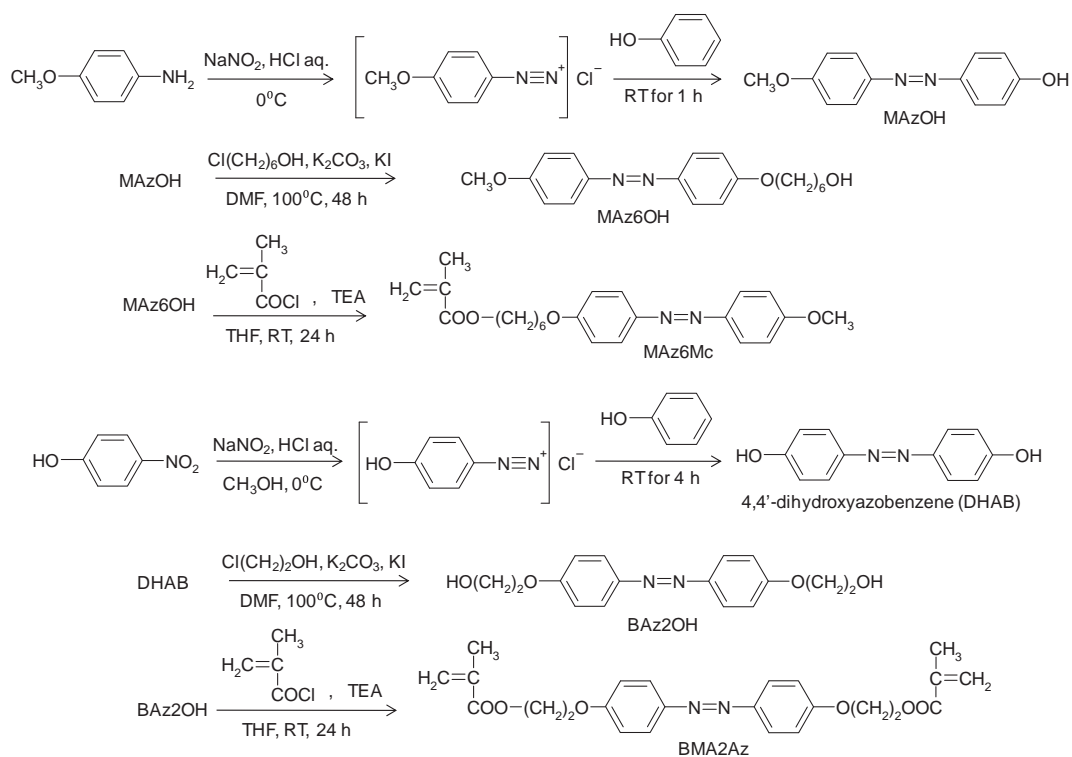
Schaeffgen and Flory first reported on synthesis of multi-chain polymer from ϵ -caprolactam using tetrabasic and octabasic carboxylic acid as a multifunctional agent [11].

However, the synthesis of star polymer remained challenging until the invention of living polymerization techniques. Living radical polymerization has recently emerged as one of the most effective synthetic routes to well-defined polymers. Among them, nitroxide mediated polymerisation (NMP) [12], atom transfer

radical polymerisation (ATRP) [13] and reversible addition–fragmentation chain transfer polymerisation (RAFT) [14] appear to be the most efficient and have been successfully applied to a large number of monomers. Very recently Matyjaszewski group reported synthesis of star polymer by a new polymerization technique known as activators regenerated by electron transfer (ARGET) ATRP [15]. However, the RAFT process involves performing conventional radical polymerisation in the presence of certain thiocarbonylthio compounds which act as highly efficient reversible addition–fragmentation chain transfer agents and provide the polymerization with living characteristics. Following RAFT polymerization, most polymer chains will have attained thiocarbonylthio and R groups as terminal groups. Synthesis of well-defined polymers of predictable molecular weights, low polydispersity indices and controlled architecture is possible through the control of the ratio of chain transfer agent (CTA) and monomer as well as polymerization conditions. Moreover, RAFT polymerization is possible in heterogeneous media. We recently reported on the synthesis of azobenzene-functionalized 2-, 3- and 4-arm azotelomers with the use of di-, tri- and tetra-functional CTAs [16].

The incorporation of azobenzene moiety into star polymers could significantly expand their potential applications due to the unique ability of azobenzene-containing polymers (azopolymers) for reversible photoisomerization between trans- and cis- isomers of the

* Corresponding author. Tel.: +81 96 342 3678; fax: +81 96 342 3679.
E-mail address: kurihara@gpo.kumamoto-u.ac.jp (S. Kurihara).



Scheme 1. Synthesis of azo-monomers MAz6Mc and BMA2Az.

chromophore, causing large changes in the polymer's size, shape, and polarity [17,18]. These unique characteristics have led to consideration of azopolymers for application in many fields such as optical data storage [19,20], liquid crystal displays [21], and holographic surface relief gratings (SRGs) [22,23]. The photoinduced trans–cis–trans photoisomerization cycle of azo chromophores upon irradiation by UV and visible light plays an important role in formation of surface relief gratings on azopolymer films. It has already been reported that azopolymers show surface relief gratings in addition to birefringence gratings upon irradiation of two polarized writing beams [24]; however, the mechanism of mass transport induced by reversible trans–cis photoisomerization remains unclarified although this phenomenon has been explored using several linear azopolymers by a number of research groups [25,26].

Additionally, only a few star azopolymers have been reported for inscription of surface relief gratings. Recently, Zhu et al reported on the synthesis of a three-arm azobenzene-containing polymers by ATRP and described the formation of surface relief gratings on their films [27]. In this article, we report the efficient synthesis of star azopolymers by RAFT process and describe the fabrication of surface relief gratings on these star azopolymer films utilizing the interference pattern of Ar⁺ laser.

2. Experimental

2.1. Synthesis of 6-(4-(4'-methoxyphenylazo)phenoxy)hexylmethacrylate, MAz6Mc

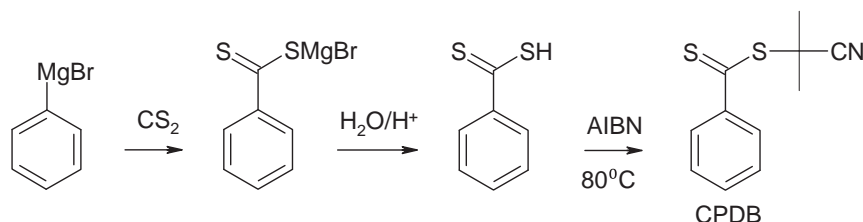
2.1.1. 4-Methoxy-4'-hydroxyazobenzene

9 g (73 mmol) of anisidine was dissolved in 300 ml of 2 M HCl; the resulting solution was cooled to 0 °C in an ice bath. 5 g (72.5 mmol) of NaNO₂ dissolved in 150 ml of water was added drop-wise to the anisidine solution to form diazonium salt. This solution was added to 6.9 g (73 mmol) of phenol dissolved in 200 ml of 2 M NaOH at 0 °C, which formed a yellow precipitate. The reaction mixture was then stirred at room temperature for 2 h. The precipitate was filtered out, recrystallized from a solution of hexane and benzene (7:2), and then dried under vacuum.

Anal. Calcd. for C₁₃H₁₂N₂O₂ (%): C, 68.41; H, 5.30; N, 12.27. Found: C, 68.53; H, 5.39; N, 12.10.

2.1.2. 4-Methoxy-4'-(6-hydroxyhexyloxy)azobenzene

To a mixture of 5 g (22.3 mmol) of 4-methoxy-4'-hydroxyazobenzene, 2.76 g (20 mmol) of K₂CO₃ and a very minute amount of KI dissolved in 100 ml of dimethylformamide (DMF), 3.05 g



Scheme 2. Synthesis of the RAFT agent 2-cyanoprop-2-yl-dithiobenzoate (CPDB).

(22.35 mmol) of 6-chlorohexanol was added. The reaction mass was heated to 100 °C and was stirred at that temperature for 24 h. The reaction mixture was then poured into water, extracted with CHCl₃, washed with water and dried over anhydrous magnesium sulphate. After removal of CHCl₃ by evaporation, the obtained liquid was poured into water. The precipitate was collected by filtration and was purified by recrystallization from methanol. The yield was 60% as solid. ¹H NMR (CDCl₃, δ): 1.0 (m, 3H, methyl), 1.3–2.0 (m, 10H, methylene), 3.4 (m, 2H, CH₂OH), 4.0–4.1 (m, 4H, CH₂OPh), 4.4 (t, 1H, OH), 6.9–7.9 (m, 8H, aromatic). Anal. Calcd. for C₁₉H₂₄N₂O₃ (%): C, 69.49; H, 7.36; N, 8.52. Found: C, 69.48; H, 7.40; N, 8.51 (Scheme 1).

2.1.3. 6-[4-(4'-Methoxyphenylazo)phenoxy]hexylmethacrylate, MAz6Mc

To a solution of 3 g (9.14 mmol) of 4-methoxy-4'-(6-hydroxyhexyloxy) azobenzene and a minute amount of hydroquinone dissolved in 50 ml of THF, slowly added were 1.85 g (18.30 mmol) of triethylamine and 1.92 g (18.30 mmol) of methacryloyl chloride at 0 °C with stirring. After stirring at room temperature for 24 h, the reaction mixture was poured into water. The precipitated product was collected and recrystallized from ethanol. Yield: 38% as solid. ¹H NMR (CDCl₃, δ): 1.0 (m, 3H, methyl), 1.4–2.0 (m, 10H, methylene), 4.0 (m, 4H, CH₂OPh), 4.2 (m, 2H, CH₂OCO), 5.8 (q, 1H, CH₂=CH), 6.1 (q, 1H, CH₂=CH), 6.4 (q, 1H, CH₂=CH), 6.9–7.9 (m, 8H, aromatic). Anal. Calcd. for C₂₃H₂₈N₂O₄ (%): C, 69.67; H, 7.11; N, 7.06. Found: C, 69.45; H, 7.08; N, 7.20.

2.2. Synthesis of difunctional azomonomer, 4,4'-methacryloylethoxyazobenzene, BMA2Az

2.2.1. Synthesis of 4,4'-dihydroxyazobenzene

20.0 g (181 mmol) of *p*-aminophenol was dissolved in 200 ml of 1 M HCl solution and was cooled to 0 °C in an ice bath. Next, 12.6 g (181 mmol) of NaNO₂ dissolved in 300 ml of water was added drop-wise to a solution of *p*-aminophenol at 0 °C. 400 ml of pre-cooled methanol was added to this diazotized solution. Then, 17.1 g (181 mmol) of phenol dissolved in 65 ml of 3 M aqueous sodium hydroxide was added drop-wise. This solution was stirred at room temperature for 2 h. Methanol was removed by evaporation. The reaction mass was then acidified with aqueous HCl, and the resulting precipitate was collected by filtration and washed with water until neutralized. The crude dihydroxyazobenzene was purified by recrystallization from ethanol/water mixture and dried under vacuum. Yield: 56.1%, Melting point: 218 °C.

2.2.2. Synthesis of 4,4'-bis(2-hydroxyethoxyazobenzene), BAz2OH

10.0 g (90.5 mmol) of 4,4'-dihydroxyazobenzene, 25.0 g (181 mmol) of potassium carbonate, 14.57 g (181 mmol) of 2-chloroethanol and a small amount of potassium iodide were dissolved in 300 ml of DMF in a flask; the reaction mass was heated to 100 °C and stirred for 48 h. After the reaction time had lapsed, a large amount of water was added; the precipitate was collected by

Table 1
Synthesis of Macro-CTA by polymerization of MAB6Mc by RAFT.

Macro-CTA	Monomer mmol	CPDB	AIBN mmol	Time h	Conversion %	Mn GPC	Mw/Mn
Macro-CTA (2.6 K)	1.3	0.05	0.034	1	13	2600	1.15
Macro-CTA (5.1 K)	1.3	0.05	0.034	5	65	5100	1.15
Macro-CTA (10 K)	1.3	0.05	0.034	20	95	10000	1.21

Solvent (Anisole): 10 ml; temperature: 60 °C; [M]/[CTA] = 15; [CTA]/[AIBN] = 1.5.

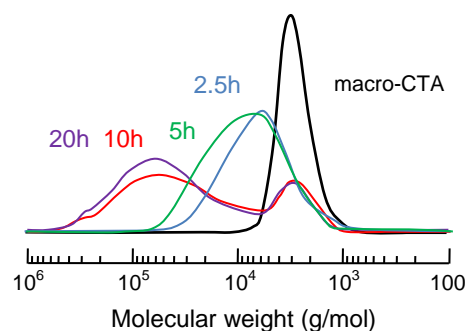


Fig. 1. GPC traces of star azopolymers at different polymerization times.

filtration, purified by recrystallization from ethyl acetate, and dried under vacuum. Yield: 24.0%, Melting point: 198 °C. Anal.: Calcd. (%): H; 6.00, C; 63.56, N; 9.27. Found(%); H; 5.95, C; 63.75, N; 8.81.

2.2.3. Synthesis of BMA2Az

13.4 g (44.3 mmol) of BAz2OH was dissolved in 250 ml of dehydrated THF and 12.3 ml (88.6 mmol) of triethylamine and 8.58 ml (88.6 mmol) of methacryloyl chloride was added to it drop-wise using a dropping funnel at 0 °C in an ice bath. The reaction mixture was then stirred at room temperature for 24 h. After the reaction time had lapsed, the reaction mixture was filtered, evaporated, dissolved in chloroform, and extracted with aqueous sodium bicarbonate solution. The extracted product was washed with water until the methacrylic acid was removed, was dried with anhydrous magnesium sulphate, and was evaporated. The solid product was purified by recrystallization from ethanol. Yield: 64.0%. Melting point: 131 °C. Anal.: Calcd. (%): H; 5.98, C; 65.74, N; 6.39. Found (%): H; 5.75, C; 65.95, N; 6.31.

2.3. Synthesis of RAFT initiator (2-cyanoprop-2-yl-dithiobenzoate; CPDB)

Dithiobenzoic acid 3.8 g (0.025 mol), DMSO 1.0 mL (0.013 mol) was added to 20 ml of ethyl acetate and was stirred under nitrogen for 7 h. Next, AIBN 3.3 g (0.017 mol) was added to the reaction solution, which was refluxed at 80 °C for 16 h. After the reaction, the solvent was removed by rotary evaporator, and crude CPDB was purified by column chromatography (developing solvent; hexane:

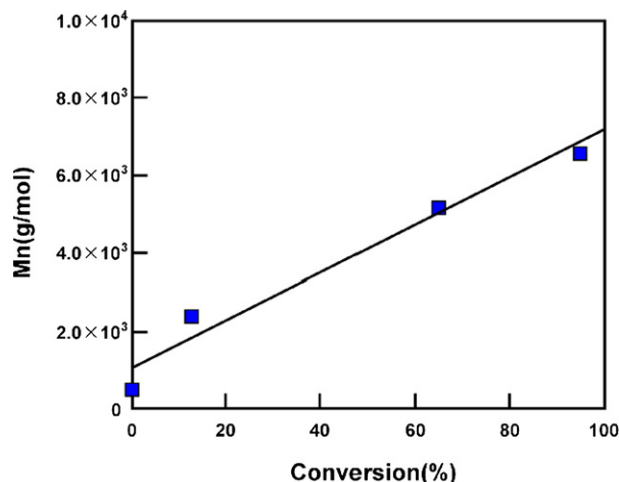


Fig. 2. Molecular weights of Macro-CTA as a function of monomer conversion in RAFT polymerization of MAz6Mc.

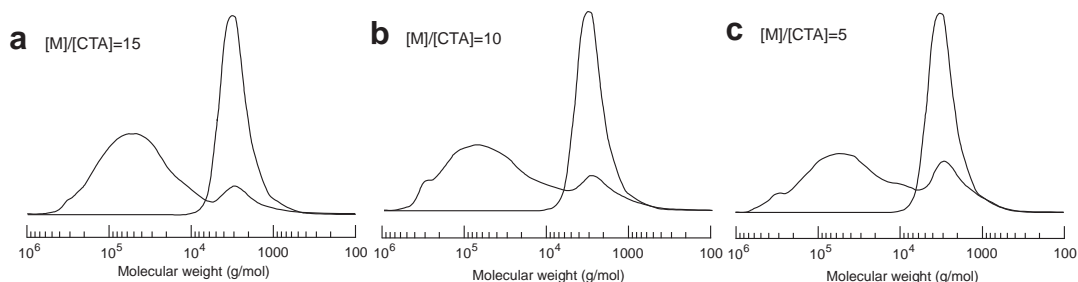


Fig. 3. GPC curves of macro-CTA2.6K (solid line) and star polymer (broken line). (a) $[M]/[CTA] = 15$, (b) $[M]/[CTA] = 10$, (c) $[M]/[CTA] = 5$.

ethyl acetate = 9:1). Yield: 16%, $^1\text{H NMR}$ (CDCl_3 , TMS): 8.0–8.1 ppm (d, 2H, C_6H_4), 7.5–7.6 ppm (m, 1H, C_6H_4); 7.3–7.4 ppm (m, 2H, C_6H_4), 1.9–2.0 (6H, CH_3) (Scheme 2).

2.4. Synthesis of Macro-CTA

0.80 g MAB6Mc, 111 μL CPDB, and 61 mg AIBN was dissolved in 10 ml anisole. Argon gas was passed through the reaction mixture for 1 h. It was then degassed through three freeze–pump–thaw cycles, sealed under vacuum, and polymerization was carried out at 60 $^\circ\text{C}$ for 20 h. Macro-CTA was precipitated by pouring the polymer solution into methanol and collected by filtration. Crude Macro-CTA was purified by chloroform/methanol re-precipitation technique and was dried under vacuum. Macro-CTAs were termed Macro-CTA(2.6) and Macro-CTA(10) on the basis of their respective molecular weights of 2600 and 10,000.

2.4.1. Synthesis of linear polymer by RAFT

Linear azopolymers of different molecular weights were also synthesized by RAFT polymerization of MAZ6Mc according to the synthetic procedures described above so as to compare their properties with star azopolymers. The characterizations of linear azopolymers are stated in Table 3.

2.5. Synthesis of star azopolymers by RAFT

Macro-CTA, monomer BMA2Az and AIBN was dissolved in 10 ml anisole; Ar gas was passed through the solution for 1 h. It was then degassed through three freeze–pump–thaw cycles and sealed under vacuum; polymerization was carried out at 60 $^\circ\text{C}$ for a pre-determined time. The polymer was precipitated in hexane, collected by filtration, and dried under vacuum. The crude star polymers were re-dissolved in THF and re-precipitated in hexane;

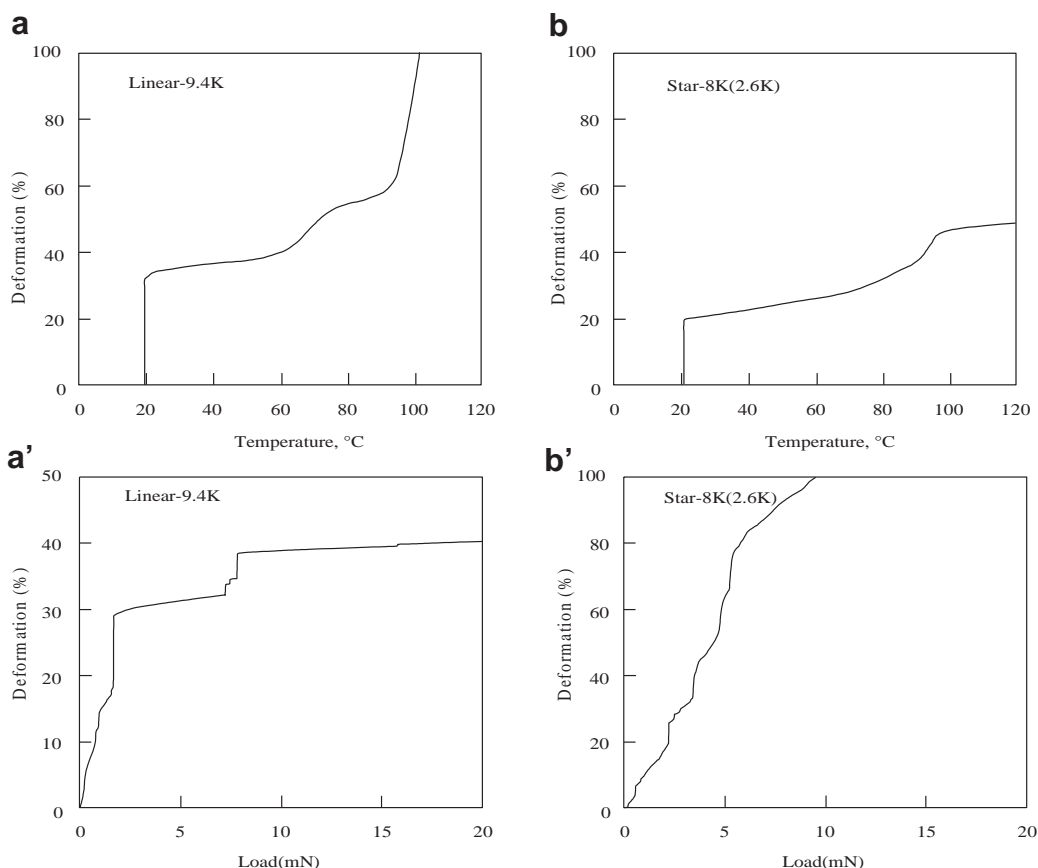


Fig. 4. TMA curves of (a,a') linear 9.4 K and (b,b') Star-8 K(2.6 K) azopolymer.

Table 2
Synthesis and characterization of star azopolymers by RAFT.

Star azopolymer	Monomer mmol	Macro-CTA mmol	AIBN mmol	Time h	Conversion %	Mn GPC	Mw/Mn	Tg °C
Star-8 K(2.6 K)	0.75	0.05	0.013	2.5	13	8000	1.15	96.1
Star-18 K(2.6 K)	0.75	0.05	0.013	5	65	18000	3.82	85.2
Star-48 K(10 K)	0.75	0.05	0.013	10	86	48000	1.87	69.6
Star-73 K(10 K)	0.75	0.05	0.013	20	95	73000	1.75	69.0

this was repeated until the star azopolymers were purified. Star azopolymers of molecular weights 8000, 18,000, 48,000 and 73,000 were designated as Star-8 K(2.6 K), Star-18 K(2.6 K), Star-48 K(10 K) and Star-73 K(10 K), respectively. The numbers in the brackets represent the molecular weights of Macro-CTAs.

2.6. Characterization

Molecular weights and molecular weight distributions of star azopolymers synthesized in this study were determined by gel permeation chromatography (GPC) equipped with JASCO RI 930 Intelligent refractive index (RI) detector and JASCO 870 UV Intelligent UV/VIS detector. The GPC was operated using Shodex KF-804F column at a flow rate of 1 ml/min THF at 40 °C and polystyrene as standard. ¹H NMR spectra of monomers and polymers were taken with a 400 MHz NMR spectrophotometer. Deuterated chloroform (Cambridge Isotope Laboratories) was used as solvent. IR spectra of star azopolymers were taken by FTIR spectrophotometer. The UV–Vis spectra of samples in THF and their films were recorded using a Shimadzu spectrophotometer. Thermal properties of star-shaped azopolymers were determined by differential scanning calorimetry (DSC) at a heating rate of 10 °C per minute, thermo-mechanical analysis (TMA), and polarized optical microscopy using Olympus BHSP polarizing microscope equipped with a Mettler FP80 and FP82 hot stage and controller. TMA experiments were carried out with a SEIKO TMA SS 100 instrument. Linear and star azopolymer films were used for TMA experiment. Reversible trans-cis photoisomerization of star-shaped azopolymers was studied by irradiating UV (366 nm) and visible light (435 nm) on their solution in THF and spin-coated films. Ar⁺ laser of (488 nm) at modest intensity was used for inscription of SRG and He–Ne laser (633 nm) was used as probe light. SRG structures were investigated by AFM (Agilent 5500, Tapping Mode) and polarized optical microscopy. The scan rate and frequency of AFM was 0.5 inch/sec and 350 kHz, respectively. The tip used in AFM was 1–10 Ohm-cm Phosphorous (n) doped Si.

3. Results and discussion

3.1. Synthesis of Macro-CTA by RAFT polymerization of MAz6Mc with CPDB initiated by AIBN

Azobenzene-functionalized monomer MAz6Mc was synthesized in good yield and purity. Linear Macro-CTA (pMAz6Mc) was synthesized by RAFT polymerization of MAz6Mc in the presence of a RAFT agent (CPDB) and AIBN initiator in anisole. CPDB was chosen as the RAFT agent because Rizzardo et al. had previously reported CPDB to be an efficient transfer agent in the polymerization of methyl methacrylate, methyl acrylate and styrene [28]. We also investigated RAFT polymerization using other RAFT agents, but no polymer with controlled molecular weight was obtained. In RAFT polymerization, which is also known as living or controlled radical polymerization, the molecular weights of the resulting polymers increase steadily with reaction time and linearly with monomer conversion.

Polymerization of MAz6Mc in the presence of the RAFT agent CPDB initiated by AIBN was carried out for 2.5, 5, 10 h; conversions of monomer determined by ¹H NMR were found to be 13%, 65% and 95%, respectively. Molecular weights of the resulting Macro-CTAs were determined by GPC and are tabulated in Table 1. It is observed that molecular weights of Macro-CTAs increased linearly with monomer conversion and slowly with polymerization time. Low polydispersity of between 1.15 and 1.21 was also exhibited by pMAz6Mc (Macro-CTAs). Thus, facile control of the polymerization is possible.

Fig. 1 illustrates typical GPC chromatograms of star azopolymers synthesized by RAFT polymerization of BMA2Az initiated by AIBN in 2.5, 5, 10 and 20 h polymerization. GPC peaks of the resulting star azopolymers clearly shift to shorter retention time (higher molecular weight) with increasing polymerization time. ¹H NMR spectra of the polymer sample after 2.5, 5, 10 and 20 h were taken and were used to calculate the conversion of monomer according to the following equation:

$$\text{Conversion} = ([M]_0 - [M]_t) / [M]_0$$

where [M]₀ is the initial concentration of monomer corresponding to the summation of integral value of vinyl group protons and benzene ring protons, and [M]_t is the concentration of monomer at time t, represented by the integral value of vinyl group protons. Using the above equation and ¹H NMR spectra of polymer samples, monomer conversion was calculated to be 16%, 65%, 86% and 95% at 2.5, 5, 10 and 20 h, respectively. Fig. 2 shows the dependence of molecular weights of star azopolymers on monomer conversion. It is clear that molecular weight of star azopolymers synthesized by RAFT polymerization increased linearly with monomer conversion, thus proving the livingness of the process.

Theoretical molecular weights of Star azopolymers can be calculated according to the following equation [29]:

$$Mn_{(\text{theo})} = [M] / [CTA] \times \text{conversion} \times MW_{\text{monomer}} + MW_{CTA}$$

where [M] is the molar concentration of monomer, [CTA] is the molar concentration of CTA, MW_{monomer} is the molecular weight of monomer, and MW_{CTA} is the molecular weight of CTA. Theoretical molecular weights of star azopolymers calculated by the above equation and molecular weights determined by GPC did not show good agreement. This may be due to the use of linear polystyrene as the standard in GPC measurement. The physical characteristics of star-shaped polymers and linear polystyrene differ in areas such as hydrodynamic volume, in which star polymers exhibit lower values.

Table 3
Molecular weights and phase transition behaviors of linear polymers.

Sample	Mn	Mw/Mn	G→S	S→N	N→I
Linear 2.6 K	2600	1.23	43	47	83
Linear 9.4 K	9400	1.52	70	88	130
Linear 31 K	31000	3.29	72	96	136
Linear 43 K	43000	1.49	116	120	145

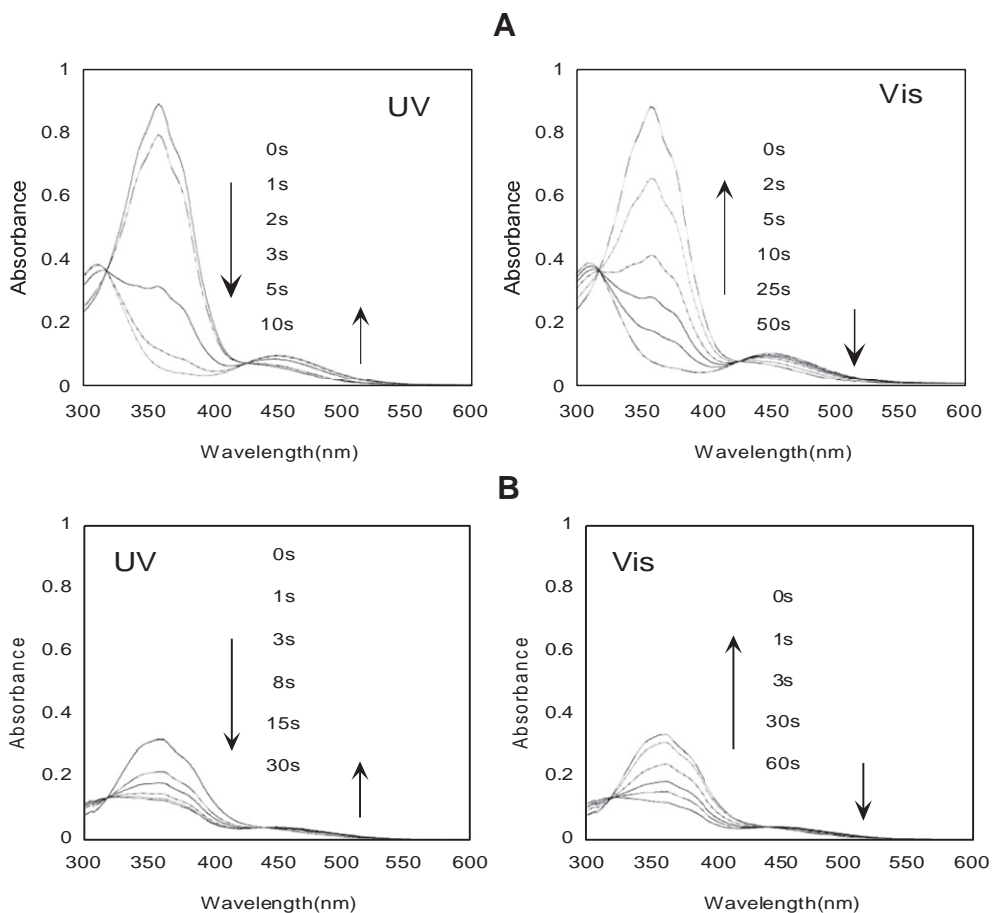


Fig. 5. Photoisomerization behaviors of Star-8 K(2.6 K) azopolymer in toluene (A), and film(B).

3.2. Effect of molar ratio of monomer to CTA ($[M]/[CTA]$)

To study the effect of the molar ratio of monomer to CTA i.e., concentration of monomer RAFT polymerization was carried out under several conditions. The polymerization was carried out for

$[M]/[CTA]$ of 5, 10, 15 and 50. Fig. 3 shows GPC chromatograms of the resulting Macro-CTA synthesized by RAFT process. Molecular weights of Macro-CTAs were found to increase with an increase in the molar ratio of monomer to CTA because of the higher conversion of monomers into polymer. However, gelation was observed at

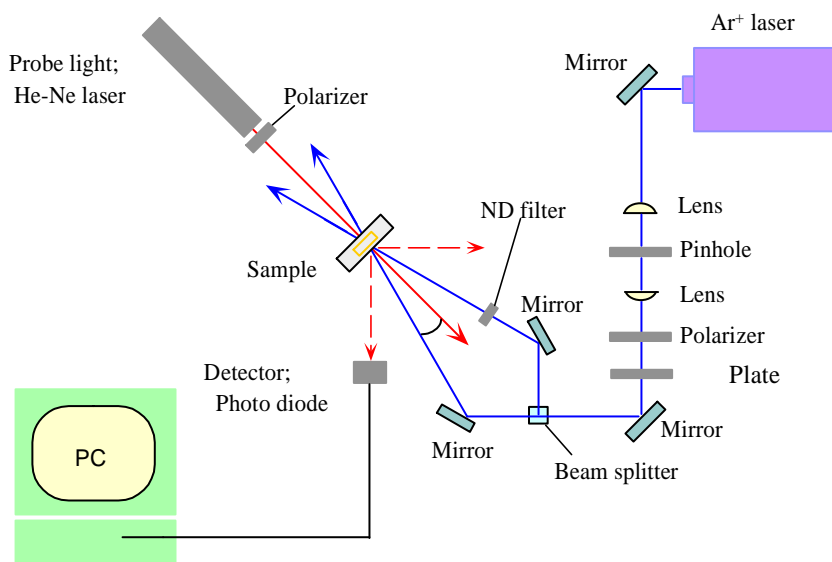


Fig. 6. Schematic diagram of experimental set-up for inscription of SRG on azopolymer films.

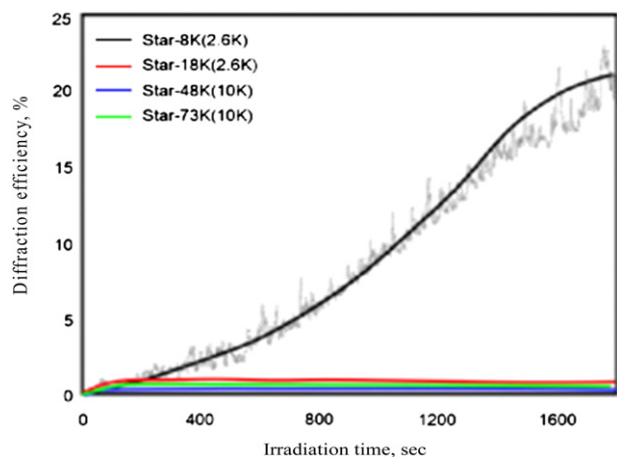


Fig. 7. Diffraction efficiencies of star azopolymers as a function of irradiation time.

the molar ratio of monomer to CTA of 50 due to the very high concentration of monomer. Similar trends were observed in other cases of synthesizing star azopolymers.

3.3. Thermomechanical analysis of linear and star polymers

Thermomechanical analysis shows specimen deformation occurrence under very low load as a function of scanned temperature. Thermomechanical analysis of linear 9.4 K polymer and Star-8 K(2.6 K) polymer films were studied to investigate changes of dimension or mechanical properties of samples subjected to a predefined temperature program and applied load. Fig. 4 shows the changes in deformation of linear 9.4 K polymer and Star-8 K(2.6 K) polymer as a function of temperature at constant applied load. Linear 9.4 K polymer showed about 40% deformation at 8 mN load, while Star-8 K(2.6 K) polymer showed 100% deformation at a similar load. Linear polymer has the structure of a polymer chain, which may be easily entangled and thus is rigid in nature. Conversely, star polymers, due to their unique characteristics, show less entanglement between molecules; also, their molecular chains are short branches that are considered to provide star polymers with high flexibility due to their low degree of freedom. In the case of linear 9.4 K polymer, no significant deformation was observed up to 65 °C (T_g); a large deformation of linear polymer film was observed at 90 °C, the phase transition temperature of smectic to nematic phase. The T_g of Star-8 K(2.6 K) polymer was 90 °C, and a large deformation was observed at that temperature.

3.4. Differential scanning calorimetric analysis

The thermal properties of linear and star azopolymers were also studied by differential scanning calorimetry (DSC) and are

described in Tables 2 and 3. Linear azopolymers showed liquid crystalline properties. Phase transition temperatures and isotropization temperatures of linear azopolymers increased with an increase in molecular weight. All linear polymers showed $G \rightarrow S \rightarrow N \rightarrow I$ phase transitions, where G, S, N and I represents glass transition, smectic, nematic and isotropic phases, respectively. On the other hand star azopolymers did not show such sharp liquid crystalline phases other than a clear glass transition temperature and isotropization temperature. As described above, the linear polymers displayed liquid crystalline properties more clearly than star polymers because the linear polymers can orient themselves in different liquid crystalline phases.

3.5. Photoresponsive properties

3.5.1. Reversible photoisomerization of star azopolymers

Photoisomerization behaviors of star azopolymers were studied in solution and film. Star azopolymer films were prepared by spin-coating of their solutions in THF onto cleaned glass substrate. The spin-coated films were air dried at room temperature. Film thickness was controlled by adjusting the concentration of solution and speed of spin-coating. Photoisomerization of the star azopolymer solution and films were carried out by UV and visible light irradiation.

Fig. 5 shows the changes in absorption spectra of Star-8 K(2.6 K) azopolymer in toluene (A) and in film (B) by UV and visible light irradiation. The UV/visible absorption spectra are characterized by a strong $\pi-\pi^*$ transition of trans-azobenzene moiety at 359 nm and a weak absorption at 450 nm, which originates from $n-\pi^*$ transition. Upon UV (366 nm; 58 mW/cm²) irradiation, absorbance at 359 nm decreased and absorbance at 450 nm increased slightly due to trans \rightarrow cis photoisomerization. Conversely, visible light irradiation (436 nm, 58 mW/cm²) caused a reverse situation to be observed. Thus, UV irradiation generates a photostationary state with a high amount of cis-isomer, while visible irradiation generates a trans-isomer rich photostationary state. The subsequent cis \rightarrow trans photoisomerization by visible light irradiation rebuilt the initial state completely, which demonstrates the reversibility of the reaction. In the case of film, photoisomerization was slower compared to that in solution. It is assumed that, because azopolymers associate or aggregate in solid film [30], the rate of photoisomerization decreased slightly.

3.5.2. Fabrication of surface relief gratings on star azopolymer films

Photofabrication of SRGs was performed on spin-coated thin films of star azopolymers. Good quality film was obtained by taking proper care in spin-coating. Polymer film thickness was controlled by changing the concentrations and speeds of coating. The spin-coated azopolymer films were kept at room temperature for 48 h or more to remove solvent. The thickness of the film was about 1 μm . An interference pattern of (CRP + CRP) Ar⁺ laser was used to

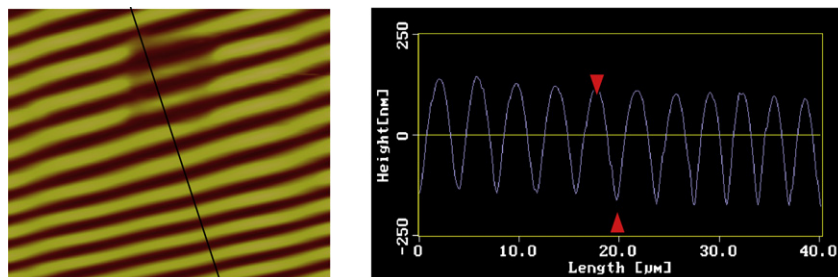


Fig. 8. AFM images of SRG on Star-8 K(2.6 K) azopolymer film by exposure to interference pattern of Ar⁺ laser for 30 min.

inscribe SRG. Relatively low light intensity of Ar⁺ laser (5 mW) was used to write the gratings in order to avoid sample damage and other possible side effects caused by high-intensity laser irradiation. Fig. 6 illustrates the optical set-up for the formation of SRGs on azopolymer films. A fringe spacing of 4 μm was maintained. Using suitable wave plates, two orthogonally polarized or p-polarized beams were used to produce the interference pattern on the polymer films. The rates of grating formation on azopolymer films was probed by measuring first-order diffraction efficiency with a He–Ne laser (100 μW), which is defined as the ratio of the intensity of the first-order diffraction beam (I_D) to that of the transmitted beam (I_T) through the film:

$$\text{Diffraction efficiency, } \eta(\%) = (I_D/I_T) \times 100$$

Fig. 7 shows diffraction efficiency of star azopolymers as a function of the irradiation time of the interference pattern of Ar⁺ laser. Diffraction efficiency of star azopolymers increased with an increase in irradiation time. A diffraction efficiency of about 20% was obtained from Star-8 K(2.6 K) polymer by irradiation of Ar⁺ laser for 30 min. The diffraction efficiencies were not so high in the case of other star polymers. Diffraction efficiency of only about 1% was obtained from Star-18 K(2.6 K), Star-48 K(10 K) and Star-73K(10 K) polymer. The sequence of diffraction efficiencies of star azopolymers are as follows: Star-8 K(2.6 K) >>> Star-18 K(2.6 K) > Star-48 K(10 K) > Star-73 K(10 K). This reveals that diffraction efficiency of star azopolymers decreased with an increase in their size and molecular weight. In the case of higher molecular weight star azopolymers, the degree of cross linking density as well as branching increases, and as a result, motion of azopolymer decreased compared to low molecular weight azopolymers. Moreover, the possibility of entanglement is lower for star azopolymers compared to their linear analogues; thus, star azopolymers showed higher diffraction efficiencies compared to linear polymers with similar molecular weights.

After grating formation, the resultant surface structure of star azopolymer films was investigated using an AFM. Fig. 8 reveals the formation of regularly spaced surface relief gratings on Star-8 K(2.6 K) azopolymer film. The modulation depths of SRGs on Star-8 K(2.6 K) film were found to be about 150 nm. SRGs formed on star azopolymer films were stable at room temperature. A detailed investigation as to both the mechanism and effects of parameters on SRG formation such as film thickness, intensity of Ar⁺ laser, and light polarization will be studied in near future to report elsewhere.

4. Conclusion

Synthesis of star azopolymers by CPDB mediated RAFT polymerization in the presence of AIBN as initiator was presented. The resultant polymers were characterized by ¹H NMR, FTIR, DSC, TMA and GPC analysis. Molecular weights of star azopolymers were found to increase linearly with conversion and slowly with polymerization time. Molecular weight distributions of the star azopolymers were also low, with some exceptions. The polymerization data prove the livingness of the RAFT process. Furthermore, thermal properties of star azopolymers were investigated by DSC,

POM and TMA. Synthesized star-shaped azopolymers showed reversible tran-cis photoisomerization in solution and film upon irradiation of UV and visible light, respectively. A diffraction efficiency as high as 20% was obtained upon exposure of Star-8 K(2.6 K) azopolymer film to interference pattern of Ar⁺ laser for 30 min. The formation of SRG on Star-8 K(2.6 K) azopolymer film occurred more rapidly than on other polymers due to its size, molecular weight and lower viscosity. The modulation depths of SRGs were about 150 nm and were found to be stable at room temperature. Thus, the star azopolymers synthesized in this study by RAFT polymerization may have potential applications in photonics and the emerging area of nanotechnology.

References

- [1] Kamigaito M, Ando T, Sawamoto M. *Chem Rev* 2001;101(12):3689–746.
- [2] Matyjaszewski K, Xia J. *Chem Rev* 2001;101(9):2921–90.
- [3] Mishra MK. *Macromolecular engineering: recent advances*. New York: Plenum Press; 1995.
- [4] Takano A, Okada M, Nose T, Fujimoto T. *Macromolecules* 1992;25(13):3596–8.
- [5] Kanaoka S, Sueoka M, Sawamoto M, Higashimura T. *J Polym Sci Polym Chem* 1993;31(10):1513–21.
- [6] Raphael E, Pincus P, Fredrickson GH. *Macromolecules* 1993;26(8):1996–2006.
- [7] Choi YK, Bae YH, Kim SW. *Macromolecules* 1998;31(25):8766–74.
- [8] Ruckenstein E, Zhang H. *Macromolecules* 1999;32(12):3979–83.
- [9] Mourey TH, Turner SR, Rubenstein M, Frechet JMJ, Hawker CJ, Wooley KL. *Macromolecules* 1992;25(9):2401–6.
- [10] Hawker CJ, Farrington P, Mackay M, Frechet JMJ, Wooley KL. *J Am Chem Soc* 1995;117(15):4409–10.
- [11] Schaeffgen JR, Flory J. *J Am Chem Soc* 1948;70(8):2709–18.
- [12] Solomon DH, Rizzardo E, Cacioli P, Hawker CJ, Bosman AW, Harth E. *Chem Rev* 2001;101(12):3661–88. US Pat. 4581429 (Chem. Abstr. 1985;102:221335).
- [13] Wang JS, Matyjaszewski K. *Macromolecules* 1995;28(23):7901–10.
- [14] (a) Chiefari J, Chong YK, Ercole F, Krstina J, Jeffery J, Le TPT, et al. *Macromolecules* 1998;31(16):5559–62; (b) Chong YK, Le PT, Moad G, Rizzardo E, Thang SH. *Macromolecules* 1999;32(6):2071–4.
- [15] Burdyska J, Cho HY, Mueller L, Matyjaszewski K. *Macromolecules* 2010;43:9227–9.
- [16] Alam MZ, Ogata T, Nonaka T, Kurihara S. *Polym Intl* 2009;58(11):1308–13.
- [17] Kumar GS, Neckers DC. *Chem Rev* 1989;89(8):1915–25.
- [18] (a) Natansohn A, Rochon P. *Chem Rev* 2002;102(11):4139–76; (b) Yoshida T, Kanaoka S, Aoshima S. *J Polym Sci Part A Polym Chem* 2005;43(18):4292–7.
- [19] Pedersen TG, Johansen PM, Pedersen HC. *J Opt A Pure Appl Opt* 2000;2:272–8.
- [20] Wu Y, Kanazawa A, Shiono T, Ikeda T, Zhang Q. *Polymer* 1999;40(17):4787–93.
- [21] Hafiz HR, Nakanishi F. *Nanotechnology* 2003;14(6):649–54.
- [22] Barrett C, Rochon P, Natansohn A. *J Chem Phys* 1998;109(4):1505–16.
- [23] Kim DY, Tripathy S, Li L, Kumar J. *Appl Phys Lett* 1995;66(10):1166–8.
- [24] Hasegawa M, Yamamoto T, Kanazawa A, Shiono T, Ikeda T. *Chem Mater* 1999;11:2764–9.
- [25] Kim DY, Li L, Jiang XL, Shivshankar V, Kumar J, Tripathy SK. *Macromolecules* 1995;28(26):8835–9.
- [26] Rasmussen PH, Ramanujam PS, Hvilsted S, Berg RH. *J Am Chem Soc* 1999;121:4738.
- [27] Zhang Y, Zhang W, Chen X, Cheng Z, Wu J, Zhu J, et al. *J Polym Sci Part A Polym Chem* 2008;46:777–89.
- [28] Rizzardo E, Chiefari J, Mayadunne RTA, Moad G, Thang SH. In: Matyjaszewski K, editor. *Controlled/living radical polymerization—Progress in ATRP, NMP and RAFT*. Washington, D.C: American Chemical Society; 2000. p. 278–97.
- [29] Benaglia M, Rizzardo E, Alberti A, Guerra M. *Macromolecules* 2005;38:3129–40.
- [30] Labarthe FL, Freiberg S, Pellerin C, Pezolet M, Natansohn A, Rochon P. *Macromolecules* 2000;33(18):6815–23.